

Geophysical Research Letters°



RESEARCH LETTER

10.1029/2023GL105190

Key Points:

- During quiet geomagnetic conditions, the regions of plasma pressure plateau are observed in the inner magnetosphere
- These regions are located at geocentric distances of 8–10 R_E forming a ring surrounding the Earth
- The localization of the plasma pressure plateau region and gaps between the Region 1 and 2 currents should be located at the same distance

Correspondence to:

I. P. Kirpichev and M. V. Stepanova, ikir@iki.rssi.ru; marina.stepanova@usach.cl

Citation:

Kirpichev, I. P., Antonova, E. E., & Stepanova, M. V. (2023). On the relationship between regions of large-scale field-aligned currents and regions of plateau in plasma pressure observed in the equatorial plane of the Earth's magnetosphere. *Geophysical Research Letters*, 50, e2023GL105190. https://doi.org/10.1029/2023GL105190

Received 26 JUN 2023 Accepted 4 SEP 2023

© 2023. The Authors.
This is an open access article under the terms of the Creative Commons
Attribution-NonCommercial-NoDerivs
License, which permits use and distribution in any medium, provided the original work is properly cited, the use is non-commercial and no modifications or adaptations are made.

On the Relationship Between Regions of Large-Scale Field-Aligned Currents and Regions of Plateau in Plasma Pressure Observed in the Equatorial Plane of the Earth's Magnetosphere

I. P. Kirpichev¹, E. E. Antonova^{1,2}, and M. V. Stepanova^{3,4}

¹Federal State Budgetary Institution of Science Space Research Institute of the Russian Academy of Sciences (IKI), Moscow, Russia, ²Skobeltsyn Institute of Nuclear Physics, Moscow State University, Moscow, Russia, ³Physics Department, Science Faculty, Universidad de Santiago de Chile, Santiago, Chile, ⁴Center for Interdisciplinary Research in Astrophysics and Space Sciences (CIRAS), Universidad de Santiago de Chile, Santiago, Chile

Abstract Since the discovery of the large-scale field-aligned currents it is widely acknowledged that gaps exist between the Region 1 (R1) and Region 2 (R2) currents in which the current values are relatively small as compared to neighboring regions. Assuming that the field-aligned currents are generated by plasma pressure gradients, we analyzed data collected by the THEMIS satellites between 2007 and 2011 to identify regions with very low plasma pressure gradients (pressure plateaus), which could be responsible for the appearance of these gaps. It was found that the pressure profiles with low radial gradients are typically located between 8 and 10 Radii around the Earth. Projections of pressure plateau regions onto ionospheric altitudes, for both individual events and on a statistical basis, coincide with the locations of gaps between Iijima and Potemra field-aligned currents. The role played by identified pressure plateaus in shaping the pattern of large-scale field-aligned currents is discussed.

Plain Language Summary Field-aligned currents that flow between the magnetosphere and ionosphere along magnetic field lines play a crucial role in magnetosphere-ionosphere interactions. Despite being discovered at the start of the space era, their origins are still subject to debate. In our current study, we have established that the observed gaps between the upward and downward currents correspond to the plateau regions of constant plasma pressure, as obtained using data from the THEMIS mission. This finding provides strong evidence in favor of the generation of field-aligned currents by plasma pressure gradients in the transition region between the dipole and tail-like geomagnetic field. This is a critical piece of information for understanding the global dynamics of Earth's magnetosphere.

1. Introduction

The presence of gaps between large-scale field-aligned currents has been observed since the early days of measuring magnetic fields aboard low-orbiting satellites (Iijima & Potemra, 1976a, 1978; Zmuda & Armstrong, 1974). For example, if we look at Figure 2 in the paper of Zmuda and Armstrong (1974), we can clearly see the presence of a gap between upward and downward currents. The gaps between current sheets are well-defined also in the global statistical distribution of large-scale field-aligned currents at ionospheric altitudes, as seen in the classic picture of Iijima and Potemra (1978).

The appearance of the IRIDIUM constellation, which comprises over 70 satellites, distributed among six circular, near-polar orbits 780 km above the earth (Anderson et al., 2000, 2008; Coxon et al., 2017, 2018; Waters et al., 2001), provides the necessary tools to obtain spatial distributions of large-scale Birkeland currents for relatively short fixed time intervals (with ten-minute resolution). This allows for the identification of gaps between current sheets of R1 and R2 of Iijima and Potemra (1978).

When the velocity of the plasma is much lower than the sound and Alfvén velocities, the plasma is near magnetostatic equilibrium (see Antonova and Ganushkina (1997), references therein and multiple other works). For isotropic plasma pressure p, the equation $[\mathbf{j} \times \mathbf{B}] = \nabla p$ applies, and this leads to the generation of a quasi-stationary system of large-scale field-aligned currents, as described by Boström (1975), Grad, (1964), Tverskoy (1982), and Vasyliunas (1970) equation.

KIRPICHEV ET AL. 1 of 9

$$j_{\parallel} = \frac{B_i}{B_e} \mathbf{b} [\nabla W \times \nabla p] \tag{1}$$

where j_{\parallel} is the density of field-aligned current (amount at the end of the field line on the ionosphere), B_i and B_e are the magnitude of the local magnetic field at ionospheric altitudes and in the plane of the geomagnetic equator, respectively, **b** is the unit vector along the magnetic field, $W = \int \frac{dl}{B}$ is the volume of the magnetic flux tube per unit flux, p is the plasma pressure.

Equation 1 indicates that when plasma pressure gradients are very small, the field-aligned current must be close to zero. The existence of gaps in the patterns of field-aligned currents led to the assumption that there are areas where these currents are not generated. However, these regions have not been extensively studied or discussed in detail. The lack of field-aligned currents may be due to the distribution of magnetic field and plasma, for which $\nabla W \parallel \nabla p$, or the presence of a plateau in plasma pressure. It was previously believed that plasma pressure smoothly increased when approaching the Earth under magnetically quiet conditions (De Michelis et al., 1999; Lui, 2003, etc.). The identification of the location of the quiet time boundary between R1 and R2 currents is a complex undertaking that requires a meticulous analysis of magnetic field observations from multiple satellites. Previous studies using CLUS-TER observations have indicated the presence of only R1 current at 19 R_F downtail (Shi et al., 2010). In contrast, Liu et al. (2016) observed both R1 and R2 currents at geocentric distances of 8–12 R_F near midnight using three THEMIS satellites. However, it is essential to note that both studies exhibit a notable scattering in the data points, potentially attributed to the frequently observed plasma sheet turbulence (Antonova & Stepanova, 2021). The location of the R1/ R2 boundary is also influenced by the current configuration of the geomagnetic field, which, in turn, exhibits strong variations depending on the solar wind and interplanetary magnetic field (IMF) conditions. Therefore, identifying regions of pressure plateau near the equatorial plane is of significant interest, as these areas could serve as a useful marker for the boundary between R1 and R2 Iijima and Potemra currents, which has not yet been accurately defined.

There have been a few studies that have identified the presence of pressure plateau regions. Specifically, Pisarenko et al. (2003), Antonova (2003), and Kirpichev (2004) found that pressure plateau regions can exist at geocentric distances of approximately 10 Earth Radii (R_E) using data from the INTERBALL/Tail Probe satellite. However, measurements taken by a single satellite do not allow for discrimination between spatial and temporal variations, making it difficult to determine if we are dealing with a spatial pressure distribution showing a plateau. Nevertheless, projecting the pressure plateau regions to the ionosphere in the nighttime sector using the Tsyganenko-2001 model (Tsyganenko, 2002) showed that the recorded pressure plateaus were mapped into an area close to the gap between the R1 and R2 field-aligned currents.

The launch of the multi-satellite THEMIS mission has allowed us to obtain measurements of plasma pressure near the equatorial plane. Previous research had primarily focused on obtaining averaged pressure profiles and their dependencies on solar wind and IMF parameters (Antonova et al., 2013, 2014; Kirpichev & Antonova, 2011; Wang et al., 2011, 2013, etc.). However, measurements taken by multiple satellites at relatively close orbits allow for the determination of temporal variations in plasma pressure. Averaged profiles cannot accurately replicate many characteristics of pressure profiles. Meanwhile, the use of two THEMIS satellites (A and D) allowed Kirpichev and Antonova (2022) to identify a pressure plateau using THEMIS data from February 2009 during the analysis of radial profiles of total (ion and electron) plasma pressure in the nighttime magnetosphere. They demonstrated that the previously detected plasma pressure plateau by Antonova (2003), Kirpichev (2004), and Pisarenko et al. (2003) is, in fact, very common at distances from 8 to 11 R_E during quiet time intervals. It was also observed that during disturbed time intervals, the plateau is destroyed and reappears when the magnetosphere returns to quiet geomagnetic conditions.

In this study, we utilized measurements from the THEMIS satellite mission to identify plasma pressure plateaus and determine their projection into ionospheric altitudes. Section 2 contains the data analysis and an example of plateau region detection. In Section 3, we present the statistical distributions of plasma plateaus and their projection to the ionospheric altitudes in comparison with (Anderson et al., 2008; Iijima & Potemra, 1976b) field-aligned currents. Finally, Section 4 is dedicated to discussion and conclusions.

2. Data Analysis

The THEMIS data from five satellites obtained between 2007 and 2011 was used to estimate the plasma pressure by calculating the second moment of the ion and electron distribution functions based on measurements of

KIRPICHEV ET AL. 2 of 9

19448007, 2023, 18, Downloaded from https://agupubs.onlinelibrary.wiley.com/doi/10.1029/2023GL105190 by Southwest Research Institute, Wiley Online Library on [03/05/2024]. See the Terms and Condit

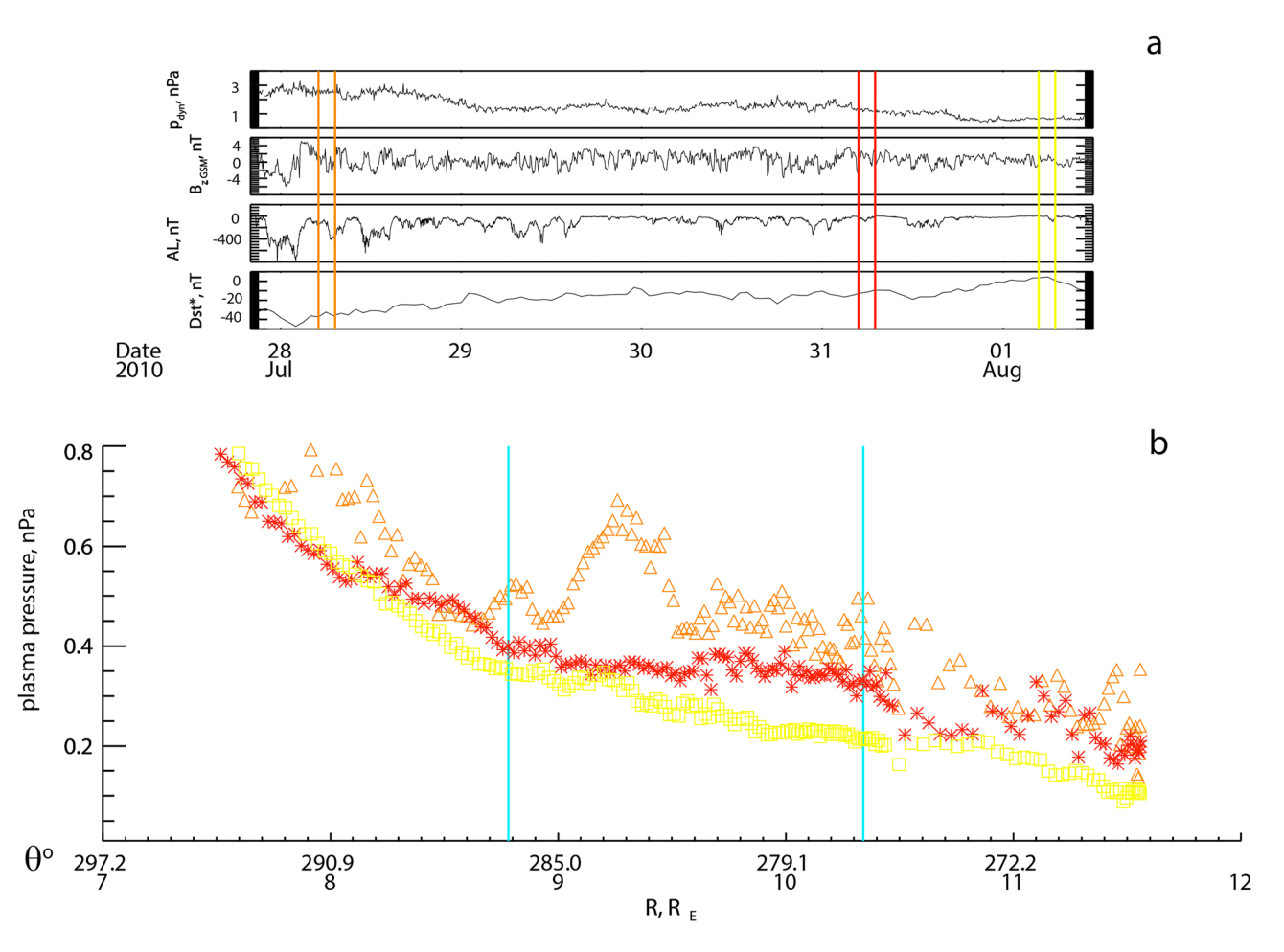


Figure 1. (a) Solar wind, interplanetary magnetic field, and AL and Dst^* indexes; (b) evolution of radial plasma profiles on 28 July–01 August 2010 (THEMIS-E) for three time intervals indicated by vertical lines in panel (a) as a function of radial distance. The azimuthal angle θ , calculated from midnight to dawn, is also indicated on the horizontal axis, alongside the radial distance.

ESA and SST instruments covering the energy range from 10 eV to 600 keV (Angelopoulos, 2008; McFadden et al., 2008; Sibeck & Angelopoulos, 2008). Full mode data corresponding to the highest possible resolution in angles and energies with a temporal resolution of up to 10 min was used. We employed the methodology implemented in the SPEDAS 5.0 software provided by the THEMIS team http://themis.ssl.berkeley.edu/ (Angelopoulos et al., 2019). To identify the plateau regions, we used the following criteria: the slope of the linear fit of pressure, normalized by its mean value, within the plateau should not exceed 0.15 in absolute value; the standard deviation should not exceed 0.15; and the absolute values of slopes for 1 R_E intervals before and after the plateau should be at least twice the absolute value of the plateau slope (see Figure 2a for some examples of plateaus).

Figure 1 illustrates a radial plasma pressure profile evolution that is typical in the formation of a plateau region. This example was taken in the evening sector of the magnetosphere on 31 July 2010. Figure 1a presents a temporal variation of the solar wind dynamic pressure, the B_z component of the IMF, and two indices of geomagnetic activity (the AL index and the ram pressure corrected Dst^* index (Burton et al., 1975)). The data was retrieved from the OMNI database (https://cdaweb.gsfc.nasa.gov). The vertical lines indicate three time intervals: from 05:00 to 07:13 UT on 28 July 2010, from 04:49 to 07:02 UT on 31 July 2010, and from 04:46 to 06:59 UT on 01 August. These intervals correspond to the distances ranging from 8.8 to 10.3 R_E of the THEMIS-E satellite, as shown by the vertical blue lines in Figure 1b, which contains three radial pressure profiles obtained from THEMIS-E measurements. The first pressure profile (orange triangles) was taken during a substorm in the recovery phase of a small magnetic storm with a minimum Dst^* of about -50 nT. Three days later, the second profile was taken, which showed a plateau in the radial pressure profile (red stars). At that time, the AL index was greater than -100 nT and Dst^* was greater than -20 nT, indicating very quiet geomagnetic conditions. The pressure

KIRPICHEV ET AL. 3 of 9

19448007, 2023, 18, Downloaded from https://agupubs.

onlinelibrary.wiley.com/doi/10.1029/2023GL105190 by Southwest Research Institute, Wiley Online Library on [03/05/2024]. See the Terms

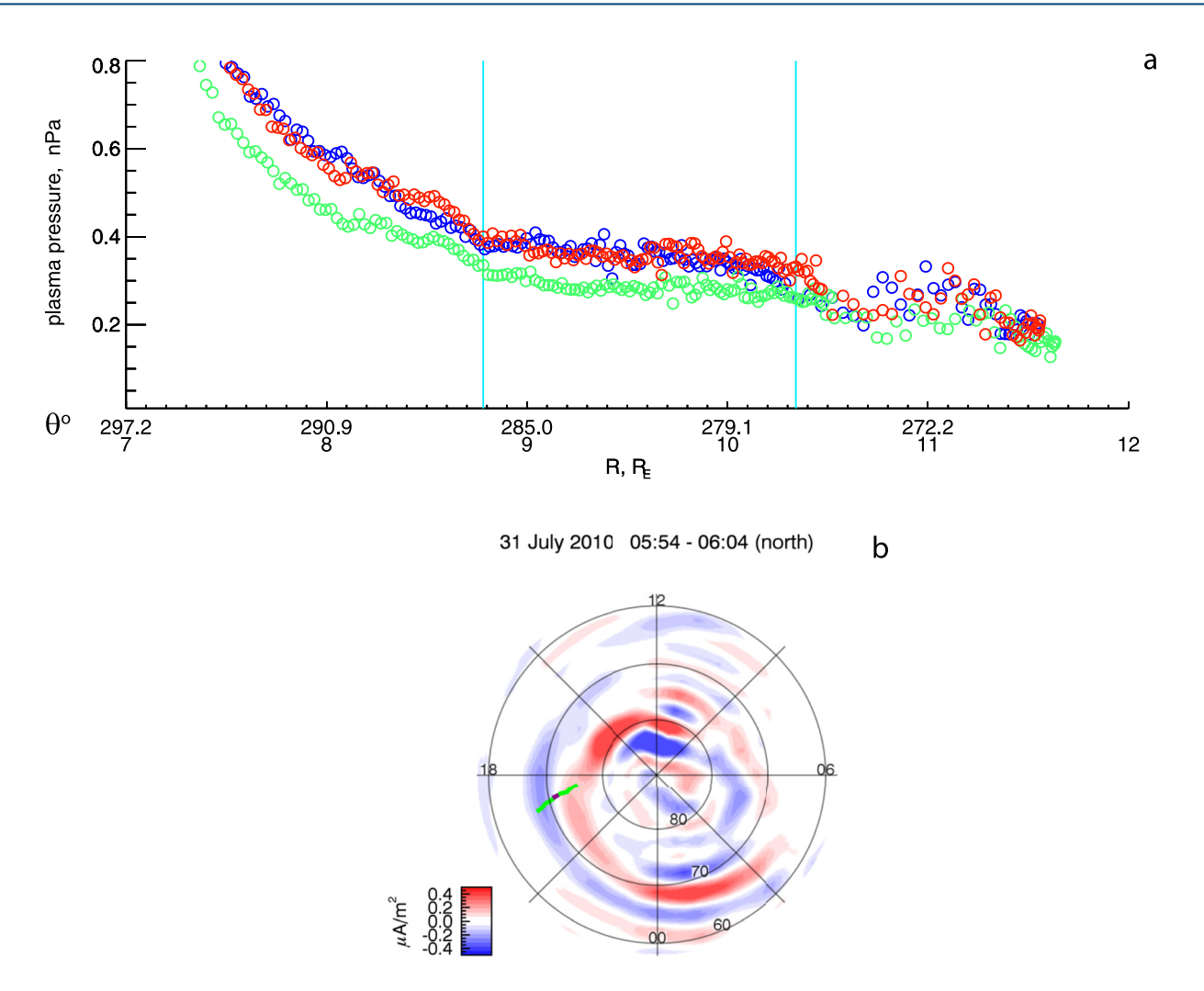


Figure 2. (a) Radial plasma profiles for THEMIS-A, -D, and -E measured on 31 July 2010; (b) Field-aligned currents obtained by AMPERE on 31 July 2010 and the projection of the plasma pressure plateau measured by THEMIS-E to the low altitudes.

decreased monotonically from Earth toward the tail of the magnetosphere until a distance of $8.8~R_E$, where it remained constant with an average value of approximately $0.35~\mathrm{nPa}$ until $10.3~R_E$ (marked by blue vertical lines). Beyond $10.3~R_E$, a more abrupt decrease was observed, marked by sharp changes in radial gradients, which is a key characteristic of all plateau crossings. The sign of the plasma pressure gradient outside the plateau region can vary. One day later, the plasma pressure evolved into a monotonically decreasing pattern (yellow squares). The lower values of plasma pressure at distances greater than $10.7~R_E$ can be attributed to a decrease in solar wind dynamic pressure from $1.3~\mathrm{on}~31~\mathrm{July}~2010$, to $0.7~\mathrm{nPa}~\mathrm{on}~01~\mathrm{August}~2010$.

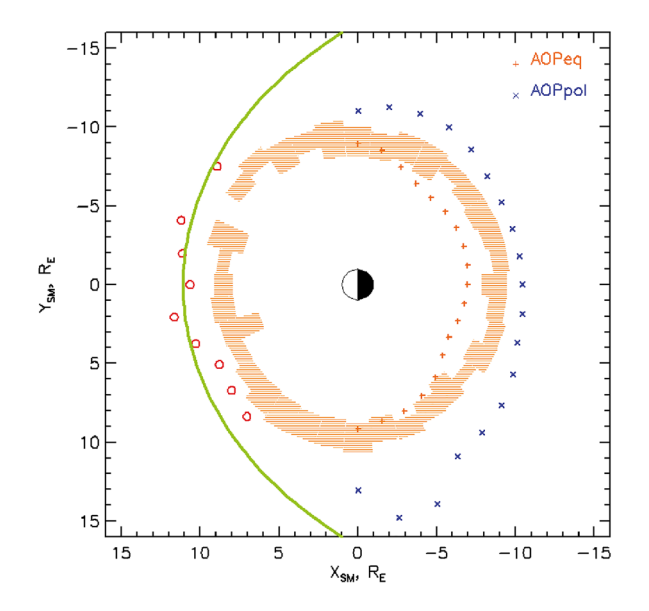
We evaluated the stability of the observed pressure plateaus by utilizing pressure profiles that were measured simultaneously by three spatially separated THEMIS satellites. A previous study conducted by Kirpichev and Antonova (2022) analyzed consecutive orbits of THEMIS-A and -D satellites intersecting the same plateau region (in the night sector) with a delay of approximately 30 min, showing its stability. Our current research confirms this result. Figure 2a illustrates three consecutive profiles that were obtained by THEMIS-E (red circles), THEMIS-A (blue circles), and THEMIS-D (green circles) on 31 July 2010. All three satellites indicate that the plateau starts at about $8.8\,R_E$, despite passing this boundary at different times (06:41 for THA, 07:04 for THD, and 07:02 UT for THE). Therefore, we can infer that the analyzed plateau region is extended in space and stable, at least within a 30-min interval.

To investigate whether plateaus affect the generation of field-aligned currents, we mapped a portion of the THEMIS-E orbit corresponding to the plateau region to the altitude of the IRIDIUM satellite, using the TA

KIRPICHEV ET AL. 4 of 9

19448007, 2023, 18, Downloaded from https://agupub

.wiley.com/doi/10.1029/2023GL105190 by South



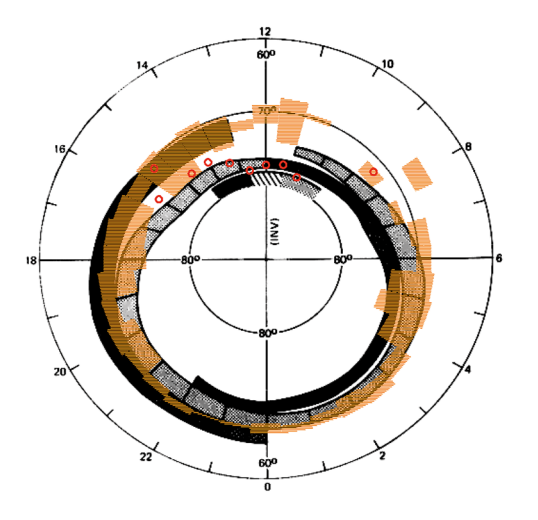


Figure 3. (a) Distribution of plasma plateau regions at the equatorial plane. The green line shows the position of the magnetopause calculated using Shue et al. (1998) model; red circles show the measured position of the magnetopause; orange "+"and blue "x" correspond to the positions of the nighttime auroral oval boundaries; (b) Global distribution of the R1 and R2 field aligned currents adopted from Iijima and Potemra (1976b) and the projection of plasma plateau regions onto the ionosphere (orange shaded areas), with red circles indicating the median positions of the magnetopause.

16 geomagnetic field model (Tsyganenko & Andreeva, 2016) and projected it along a field line to an altitude (northern hemisphere) of approximately 800 km in geographic coordinates (GEO). We then transformed the data into the AACGM system (Shepherd, 2014) and determined the corresponding invariant latitude and MLT. We then superimposed this data with the distribution of field-aligned currents, reconstructed using AMPERE tools. The data were collected on 31 July 2010, between 05:54 and 06:04 UT while THEMIS-E was located in the center of the plateau. Red regions indicate currents flowing away from the ionosphere, while blue regions represent currents flowing into the ionosphere. Figure 2b shows the results of projecting the entire plateau area, which is bounded by vertical blue lines in Figures 1b and 2a. The green curve represents the projection, and the dark magenta segment on the green curve corresponds to the interval of the THEMIS-E passage from 05:54 to 06:04 UT on 31 July 2010. The center of the plateau area projection coincides with the region of the gap between the current sheets in the AMPERE image. Although the distribution pattern of currents changes in close time intervals, the gap between the current sheets remains. The coincidence of the position of the plasma pressure plateau and the region where field-aligned currents at ionospheric altitudes are absent supports the assumption made in the introduction about the formation of the gap region between the Iijima and Potemra R1 and R2 currents as a result of the formation of plateau regions in radial pressure distribution.

3. Statistical Distribution of the Plasma Plateau Regions

After analyzing pressure data from all MLT during quiet geomagnetic conditions (|Dst| < 20 nT, |AL| < 200 nT), we identified 580 orbits containing a plateau region, and determined their equatorial and polar boundaries. To visualize the spatial distribution of plateau regions in the equatorial plane, we divided the equatorial plane into 36 sectors. For each sector, the averaged equatorial (closer to Earth) and polar (farther from Earth) boundaries were determined based on their median values. The final distribution of plasma plateau regions (orange shaded areas) in the XY plane of the SM coordinate system is given in Figure 3a.

To understand the position of the plateau regions relative to other boundaries, we identified the location of the magnetopause for all satellite passes in the day sectors. In Figure 3a, the red circles represent the median positions of the magnetopause for each sector, determined from corresponding dayside passes with a clearly identified plateau region. We determined the position by looking for a change in the shear angle that occurred during the transition from the inner magnetosphere to the magnetosheath, following the methodology of Phan et al. (1994). We also included the position of the magnetopause, calculated using the Shue model (Shue et al., 1998) for the mean values of solar wind parameters for the entire period for which plateau statistics were collected (green line). Additionally, we reproduced the projec-

tions onto the equatorial plane of the nighttime polar (blue "x") and equatorial (orange "+") boundaries of the quiet auroral oval obtained by Kirpichev et al. (2016). As a result, we can see that the polar boundary of the plateau region for day sectors is always located at least one R_E away from the magnetopause. On the night side, the plateau region falls between the polar and equatorial boundaries of the auroral oval. To compare the location of plateau regions with the averaged distribution of field-aligned currents obtained by Iijima and Potemra (Iijima & Potemra, 1976b), we mapped the boundaries of each plateau obtained along the satellite orbit onto an altitude of 800 km, using the TA 16 model as described in the Data Analysis section. After that we calculated the median position for equatorial and polar boundaries for each MLT sector. Figure 3b shows the overlap between R1 and R2 field-aligned currents adapted from Iijima and Potemra (1976b) and the projection of plasma plateau regions

KIRPICHEV ET AL. 5 of 9

onto the ionosphere (orange shaded areas). The median positions of the magnetopause projection are also indicated as red circles. It is surprising that there is a coincidence between the plateau regions and the gap between the upward and downward current regions in sectors from 14 to 24 MLT, considering that we are dealing with the averaged picture of both field-aligned currents and plateau regions. The projection of the median positions of the magnetopause, except for the sector of 13–16 MLT, is located toward the poles from the plateau region. The picture is more diffuse in sectors from 0 to 9 MLT. Nonetheless, it is possible to see that the projection of the plateau region practically does not exceed the boundaries of the field-aligned current regions in the Iijima and Potemra (1976b) pictures.

Recent studies have revealed a strong correlation between the IMF orientation and the distribution of field-aligned currents. In particular, Anderson et al. (2008) developed a statistical model of the IRIDIUM Birkeland currents based on the clock angle (ψ), which is defined as $\psi = \arctan(B_y, B_z)$, where B_y and B_z are the GSM projections of the averaged IMF. They divided the data set into eight subsets, each centered at $\psi = 0^\circ, \pm 45^\circ, \pm 90^\circ, \pm 135^\circ$, and $|\psi| = 180^\circ$, with a width of 45°. In our study, we applied the same criterion and divided our data accordingly. For each subset, we calculated the projections of the plasma plateau regions onto the ionosphere.

Figure 4 illustrates the superposition of the statistical distribution of the IRIDIUM Birkeland upward currents (indicated in red) and downward currents (indicated in blue), adapted from Anderson et al. (2008), along with the projections of the pressure plateau regions denoted by shaded orange areas. The central panel of Figure 4 displays arrows indicating the orientation of the IMF. The labels "+Z" and "+Y" correspond to IMF northward (N) and eastward (E) at the subsolar dayside magnetopause, respectively. Each panel is labeled to indicate the center clock angle bin, such as (SW) for south-west, -Z, and -Y. Notably, we observe a significant alignment between the pressure plateau regions and the gaps in the field-aligned currents across all IMF orientations.

4. Conclusions

A statistical study of 580 events of nearly constant pressure along a satellite orbit, occurring during quiet geomagnetic conditions, revealed that the plateau regions in the equatorial plane form a nearly circular structure around the Earth at geocentric distances of approximately 8–10 R_F. These plateaus are separated from the magnetopause at the subsolar point by a distance of approximately $2 R_F$. The formation of these plateaus is due to the evolution of pressure profiles sensitive to geomagnetic conditions. For negative X_{SM} , the plateau regions are localized within the projection of the quiet auroral oval boundaries onto the equatorial plane. The projection of the plateau region onto ionospheric altitudes accurately matches with the gap between the R1 and R2 currents, both for individual events using maps of AMPERE field-aligned currents and for averaged distributions of currents obtained by Iijima and Potemra (1976b) and Anderson et al. (2008). This result supports the idea that large-scale field-aligned currents in the magnetosphere are generated due to pressure gradients of the plasma, as formulated in many works (see, e.g., Wolf, 1983; Toffoletto et al., 2003, etc.), and verified experimentally (see Xing et al. (2009) and references therein). Our findings indicate the absence of a pressure gradient along the trajectory of the satellite. However, it is important to note that satellite trajectories are never perfectly radial. The presence of a plateau suggests that both the radial and azimuthal components of the pressure gradient are nearly zero. This is because it would be unlikely for all analyzed trajectories to align precisely along a line of constant pressure if there were significant radial and azimuthal pressure gradients present. The location of boundaries of the large-scale field-aligned current regions in projection to the equatorial plane had not been identified until now, and our work puts us a step closer to resolving this question. The obtained results provide additional evidence for the plasma pressure gradient mechanism of field-aligned current generation. At the same time, by identifying the plateau region at geocentric distances of approximately $8-10 R_F$ during quiet geomagnetic conditions, we can conclude that the boundaries between the R1 and R2 currents should also be situated at the same distance. This proximity aligns with the findings of Liu et al. (2016). It is important to note, however, that even during quiet geomagnetic conditions, the configuration of the magnetosphere is sensitive to solar wind parameters, for example, the dynamic pressure. This study did not explicitly consider them, which might explain the discrepancies observed with previous studies. In the case of the dayside magnetosphere, the plateau region is localized at distances for which it is commonly assumed that we deal with the dayside continuation of the plasma sheet. Nonetheless, there is strong evidence that this region corresponds to the external part of the ring current (see Antonova et al. (2018), and references therein). Our current results show that, in fact, the gaps between the borders of the field-aligned current regions form a ring structure surrounding the Earth.

KIRPICHEV ET AL. 6 of 9

Research Institute, Wiley Online Library on [03/05/2024]. See the Terms

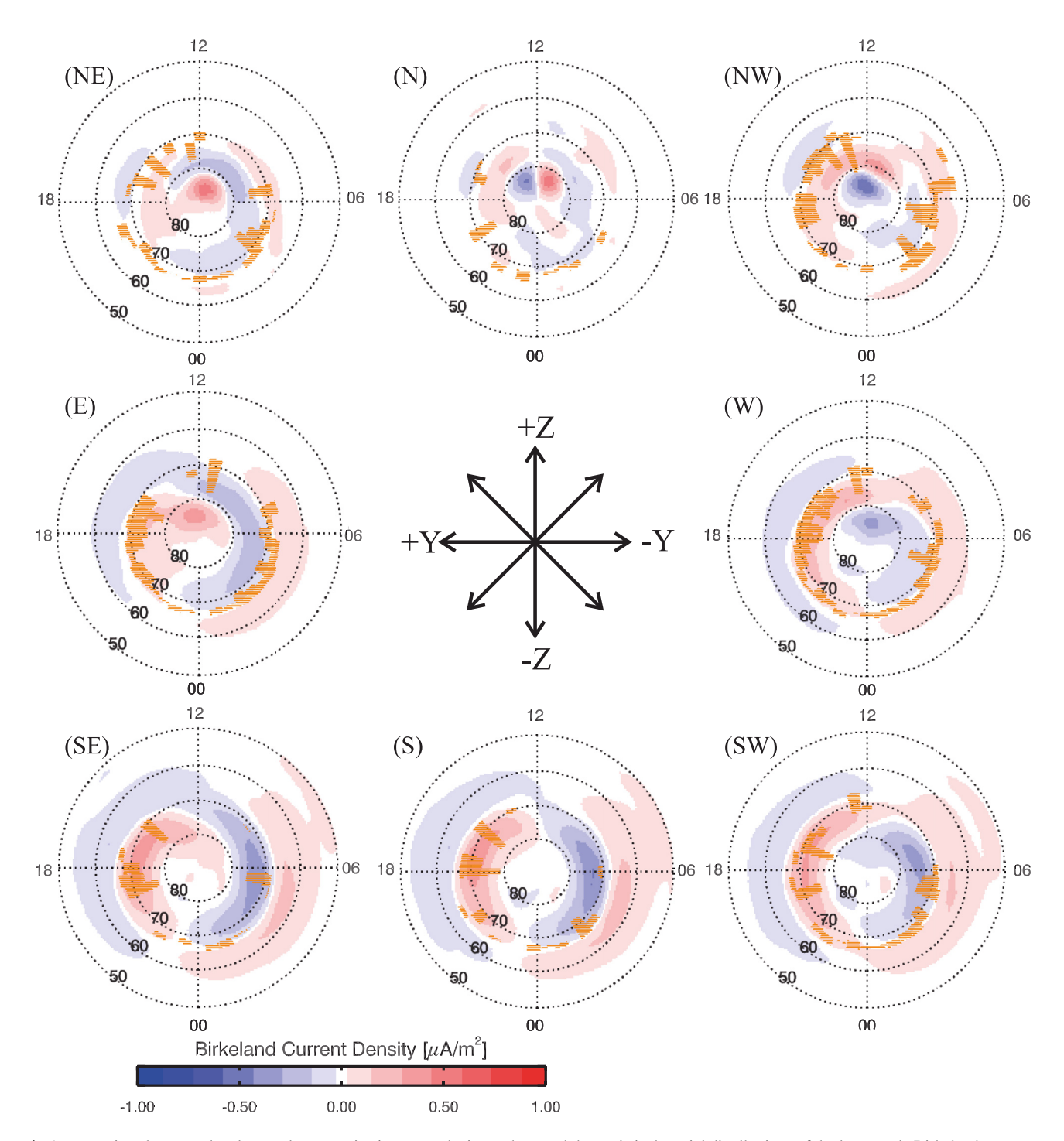


Figure 4. A comparison between the plasma plateau projections onto the ionosphere and the statistical spatial distributions of the large-scale Birkeland currents, adopted from Anderson et al. (2008).

Data Availability Statement

The data used in this work were downloaded from sites http://themis.ssl.berkeley.edu/data_retrieval.shtml, https://ampere.jhuapl.edu/download/ and https://cdaweb.gsfc.nasa.gov/pub/data/omni/.

KIRPICHEV ET AL. 7 of 9



Geophysical Research Letters

10.1029/2023GL105190

Acknowledgments

The authors acknowledge NASA Contract NAS5-02099 and V. Angelopoulos for the use of THEMIS mission data, as well as D. Larson and R.P. Lin for SST data, C.W. Carlson and J.P. McFadden for ESA data, K.H. Glassmeier, U. Auster, and W. Baumjohann for FGM data provided under the lead of the Technical University of Braunschweig and with financial support through the German Ministry for Economy and Technology and the German Center for Aviation and Space (DLR) under Contract 50 OC 0302. We thank the AMPERE team and the AMPERE Science Data Center for providing data products derived from the IRIDIUM Communications constellation. enabled by support from the National Science Foundation. MS was supported by the FONDECYT 1211144 research

References

- Anderson, B. J., Korth, H., Waters, C. L., Green, D. L., & Stauning, P. (2008). Statistical Birkeland current distributions from magnetic field observations by the Iridium constellation. *Annales Geophysicae*, 26(3), 671–687. https://doi.org/10.5194/angeo-26-671-2008
- Anderson, B. J., Takahashi, K., & Toth, B. A. (2000). Sensing global Birkeland currents with Iridium engineering magnetometer data. Geophysical Research Letters, 27(24), 4045–4048. https://doi.org/10.1029/2000GL000094
- Angelopoulos, V. (2008). The THEMIS mission. Space Science Reviews, 141(1-4), 5-34. https://doi.org/10.1007/s11214-008-9336-1
- Angelopoulos, V., Cruce, P., Drozdov, A., Grimes, E. W., Hatzigeorgiu, N., King, D. A., et al. (2019). The space physics environment data analysis system (SPEDAS). Space Science Reviews, 215(1), 9. https://doi.org/10.1007/s11214-018-0576-4
- Antonova, E. E. (2003). Investigations of the hot plasma pressure gradients and the configuration of magnetospheric currents from Interball. Advances in Space Research, 31(5), 1157–1166. https://doi.org/10.1016/S0273-1177(03)00077-2
- Antonova, E. E., & Ganushkina, N. Y. (1997). Azimuthal hot plasma pressure gradients and dawn-dusk electric field formation. *Journal of Atmospheric and Solar-Terrestrial Physics*, 59(11), 1343–1354. https://doi.org/10.1016/S1364-6826(96)00169-1
- Antonova, E. E., Kirpichev, I. P., & Stepanova, M. V. (2014). Plasma pressure distribution in the surrounding the Earth plasma ring and its role in the magnetospheric dynamics. *Journal of Atmospheric and Solar-Terrestrial Physics*, 115, 32–40. https://doi.org/10.1016/j.jastp.2013.12.005
- Antonova, E. E., Kirpichev, I. P., Vovchenko, V. V., Stepanova, M. V., Riazantseva, M. O., Pulinets, M. S., et al. (2013). Characteristics of plasma ring, surrounding the Earth at geocentric distances 7–10 R_E, and magnetospheric current systems. *Journal of Atmospheric and Solar-Terrestrial Physics*, 99, 85–91. https://doi.org/10.1016/j.jastp.2012.08.013
- Antonova, E. E., & Stepanova, M. V. (2021). The impact of turbulence on physics of the geomagnetic tail. Frontiers in Astronomy and Space Sciences, 8, 622570. https://doi.org/10.3389/fspas.2021.622570
- Antonova, E. E., Stepanova, M. V., Kirpichev, I. P., Ovchinnikov, I. L., Vorobjev, V. G., Yagodkina, O. I., et al. (2018). Structure of magnetospheric current systems and mapping of high latitude magnetospheric regions to the ionosphere. *Journal of Atmospheric and Solar-Terrestrial Physics*, 177, 103–114. https://doi.org/10.1016/j.jastp.2017.10.013
- Boström, R. (1975). Mechanisms for driving birkeland currents. In B. Hultqvist & L. Stenflo (Eds.), *Physics of the hot plasma in the magneto-sphere* (pp. 341–362). Springer US. https://doi.org/10.1007/978-1-4613-4437-7_16
- Burton, R. K., McPherron, R. L., & Russell, C. T. (1975). An empirical relationship between interplanetary conditions and Dst. *Journal of Geophysical Research*, 80(31), 4204–4214. https://doi.org/10.1029/JA080i031p04204
- Coxon, J. C., Milan, S. E., & Anderson, B. J. (2018). A review of birkeland current research using ampere. In *Electric currents in geospace and beyond* (pp. 257–278). American Geophysical Union (AGU). https://doi.org/10.1002/9781119324522.ch16
- Coxon, J. C., Rae, I. J., Forsyth, C., Jackman, C. M., Fear, R. C., & Anderson, B. J. (2017). Birkeland currents during substorms: Statistical evidence for intensification of regions 1 and 2 currents after onset and a localized signature of auroral dimming. *Journal of Geophysical Research: Space Physics*, 122(6), 6455–6468. https://doi.org/10.1002/2017JA023967
- De Michelis, P., Daglis, I. A., & Consolini, G. (1999). An average image of proton plasma pressure and of current systems in the equatorial plane derived from AMPTE/CCE-chem measurements. *Journal of Geophysical Research*, *104*(A12), 28615–28624. https://doi.org/10.1029/1999JA900310
- Grad, H. (1964). Some new variational properties of hydromagnetic equilibria. The Physics of Fluids, 7(8), 1283–1292. https://doi.org/10.1063/1.1711373
- lijima, T., & Potemra, T. A. (1976a). The amplitude distribution of field-aligned currents at northern high latitudes observed by Triad. *Journal of Geophysical Research*, 81(13), 2165–2174. https://doi.org/10.1029/JA081i013p02165
- Iijima, T., & Potemra, T. A. (1976b). Field-aligned currents in the dayside cusp observed by Triad. Journal of Geophysical Research, 81(34), 5971–5979. https://doi.org/10.1029/JA081i034p05971
- Iijima, T., & Potemra, T. A. (1978). Large-scale characteristics of field-aligned currents associated with substorms. *Journal of Geophysical Research*, 83(A2), 599–615. https://doi.org/10.1029/JA083iA02p00599
- Kirpichev, I. P. (2004). Distribution of plasma pressure in the geomagnetic tail in the transition region from dipole to quasidipole and stretched magnetic field lines: Events on October 13, 1995 and March 13, 1996. Cosmic Research, 42(4), 338–348. https://doi.org/10.1023/B:COSM.0000039732.86850.78
- Kirpichev, I. P., & Antonova, E. E. (2011). Plasma pressure distribution in the equatorial plane of the Earth's magnetosphere at geocentric distances of 6–10 R_E according to the international THEMIS mission data. *Geomagnetism and Aeronomy*, 51(4), 450–455. https://doi.org/10.1134/S0016793211040049
- Kirpichev, I. P., & Antonova, E. E. (2022). A plasma pressure plateau in the night sector of the Earth's magnetosphere and its stability. *Geomagnetism and Aeronomy*, 62(S1), S28–S39. https://doi.org/10.1134/S001679322260059X
- Kirpichev, I. P., Yagodkina, O. I., Vorobjev, V. G., & Antonova, E. E. (2016). Position of projections of the night side auroral oval equator-ward and poleward edges in the magnetosphere equatorial plane. *Geomagnetism and Aeronomy*, 56(4), 407–414. https://doi.org/10.1134/S001679321604006X
- Liu, J., Angelopoulos, V., Chu, X., & McPherron, R. L. (2016). Distribution of region 1 and 2 currents in the quiet and substorm time plasma sheet from THEMIS observations. *Geophysical Research Letters*, 43(15), 7813–7821. https://doi.org/10.1002/2016GL069475
- Lui, A. T. Y. (2003). Inner magnetospheric plasma pressure distribution and its local time asymmetry. Geophysical Research Letters, 30(16), 1846. https://doi.org/10.1029/2003GL017596
- McFadden, J. P., Carlson, C. W., Larson, D., Bonnell, J., Mozer, F., Angelopoulos, V., et al. (2008). THEMIS ESA first science results and performance issues. Space Science Reviews, 141(1-4), 477-508. https://doi.org/10.1007/s11214-008-9433-1
- Phan, T. D., Paschmann, G., Baumjohann, W., Sckopke, N., & Lühr, H. (1994). The magnetosheath region adjacent to the dayside magnetopause: AMPTE/IRM observations. *Journal of Geophysical Research*, 99(A1), 121–141. https://doi.org/10.1029/93JA02444
- Pisarenko, N., Budnik, E., Ermolaev, Y., Kirpichev, I., Lutsenko, V., Morozova, E., & Antonova, E. (2003). The main features of the ion spectra variations in the transition region from dipole to tailward stretched field lines. *Advances in Space Research*, 31(5), 1347–1352. (Plasma Processes in the Near-Earth Space: Interball and Beyond). https://doi.org/10.1016/S0273-1177(03)00018-8
- Shepherd, S. G. (2014). Altitude-adjusted corrected geomagnetic coordinates: Definition and functional approximations. *Journal of Geophysical Research: Space Physics*, 119(9), 7501–7521. https://doi.org/10.1002/2014JA020264
- Shi, J. K., Cheng, Z. W., Zhang, T. L., Dunlop, M., Liu, Z. X., Torkar, K., et al. (2010). South-north asymmetry of field-aligned currents in the magnetotail observed by cluster. *Journal of Geophysical Research*, 115(A7), A07228. https://doi.org/10.1029/2009JA014446
- Shue, J. H., Song, P., Russell, C. T., Steinberg, J. T., Chao, J. K., Zastenker, G. N., et al. (1998). Magnetopause location under extreme solar wind conditions. *Journal of Geophysical Research*, 103(A8), 17691–17700. https://doi.org/10.1029/98JA01103

KIRPICHEV ET AL. 8 of 9

- Sibeck, D. G., & Angelopoulos, V. (2008). THEMIS science objectives and mission phases. Space Science Reviews, 141(1-4), 35-59. https://doi.org/10.1007/s11214-008-9393-5
- Toffoletto, F., Sazykin, S., Spiro, R., & Wolf, R. (2003). Inner magnetospheric modeling with the rice convection model. In A. C.-L. Chian, I. H. Cairns, S. B. Gabriel, J. P. Goedbloed, T. Hada, M. Leubner, et al. (Eds.), *Advances in space environment research: Volume i* (pp. 175–196). Springer Netherlands. https://doi.org/10.1007/978-94-007-1069-6_19
- Tsyganenko, N. A. (2002). A model of the near magnetosphere with a dawn-dusk asymmetry 1. Mathematical structure. *Journal of Geophysical Research*, 107(A8), SMP12-1–SMP12-15. https://doi.org/10.1029/2001JA000219
- Tsyganenko, N. A., & Andreeva, V. A. (2016). An empirical RBF model of the magnetosphere parameterized by interplanetary and ground-based drivers. *Journal of Geophysical Research: Space Physics*, 121(11), 10786–10802. https://doi.org/10.1002/2016JA023217
- Tverskoy, B. A. (1982). On magnetospheric field-aligned currents. Geomagnetism and Aeronomy, 22, 991–995.
- Vasyliunas, V. M. (1970). Mathematical models of magnetospheric convection and its coupling to the ionosphere. In B. M. McCormac (Ed.), *Particles and fields in the magnetosphere* (pp. 60–71). Springer Netherlands.
- Wang, C. P., Gkioulidou, M., Lyons, L. R., Wolf, R. A., Angelopoulos, V., Nagai, T., et al. (2011). Spatial distributions of ions and electrons from the plasma sheet to the inner magnetosphere: Comparisons between THEMIS-geotail statistical results and the rice convection model. *Journal of Geophysical Research*, 116(A11), A11216. https://doi.org/10.1029/2011JA016809
- Wang, C.-P., Yue, C., Zaharia, S., Xing, X., Lyons, L., Angelopoulos, V., et al. (2013). Empirical modeling of plasma sheet pressure and three-dimensional force-balanced magnetospheric magnetic field structure: 1. Observation. *Journal of Geophysical Research: Space Physics*, 118(10), 6154–6165. https://doi.org/10.1002/jgra.50585
- Waters, C. L., Anderson, B. J., & Liou, K. (2001). Estimation of global field aligned currents using the iridium® system magnetometer data. Geophysical Research Letters, 28(11), 2165–2168. https://doi.org/10.1029/2000GL012725
- Wolf, R. A. (1983). The quasi-static (slow-flow) region of the magnetosphere. In R. L. Carovillano & J. M. Forbes (Eds.), *Solar-terrestrial physics* (pp. 303–368). Springer Netherlands.
- Xing, X., Lyons, L. R., Angelopoulos, V., Larson, D., McFadden, J., Carlson, C., et al. (2009). Azimuthal plasma pressure gradient in quiet time plasma sheet. *Geophysical Research Letters*, 36(14), L14105. https://doi.org/10.1029/2009GL038881
- Zmuda, A. J., & Armstrong, J. C. (1974). The diurnal flow pattern of field-aligned currents. *Journal of Geophysical Research*, 79(31), 4611–4619. https://doi.org/10.1029/JA079i031p04611

KIRPICHEV ET AL. 9 of 9